

Design and Parameter Optimization of Torsion Shock Absorber for Fracturing Pump Crankshaft System

Zhongyan Liu^{1,2}, Fangjian Chen^{1,2}, Wensheng Xiao^{1,2*}, Chengzhi Xue^{1,2}, Hanchuan Wu³,
Qingqun Wang³

¹ College of Mechanical and Electronic Engineering, China University of Petroleum, Qingdao, China

² National Engineering Laboratory for Marine Geophysical and Exploration Equipment, Qingdao, China

³ Sinopec Petroleum Machinery Co., Ltd., Wuhan, China

*Corresponding author: xiaows@upc.edu.cn

Keywords: Fracturing Pump Crankshaft System, Torsion Shock Absorber, Control of Torsional Vibration, Parameter Optimization.

Abstract: The torsional vibration is an important component of the fracturing pump truck, and it is also one of the important sources of the vibration noise. It is necessary to study the control of the torsional vibration of the fracturing pump crankshaft system. In this paper, a torsional shock absorber with silicone oil damping is designed for the fracturing pump crankshaft system to reduce the torsional vibration of the system. The inertia ring of the torsional shock absorber is designed by the empirical method. The preliminary parameters of the torsional shock absorber are obtained and the appropriate type of silicone oil is selected. Then, based on the numerical method and the standard particle swarm optimization (PSO) algorithm, the torsional vibration responses of the system before and after optimizing the torsional shock absorber are analyzed and compared. The statistical results indicate that the optimal torsional shock absorber is more effective for the torsional vibration reduction of system.

1. Introduction

The fracture, which is the key technology to realize the development of the shale oil and gas, is usually used to increase the reservoir permeability and the productivity of oil wells [1]. The fracturing pump truck is the crucial equipment for the fracturing technology, whose function is to fracture the formation by injecting fracturing fluids with high pressure and large displacement and squeeze the proppant into the formation fracture.

The 3000HP fracturing pump truck has been widely applied to the large-scale fracturing operations in North America. The increase of the pressure and displacement of the fracturing pump puts forward higher requirements for the performance and control of the torsional vibration of the transmission shaft in the fracturing pump truck. The explosive force of gas and reciprocating inertia force generated by the engine under high power and high operating pressure could result in sharp increase of the amplitude of each harmonic exciting torque, which means that the torsional vibration obviously appears in the transmission shaft in the fracturing pump truck.

Zhu et al. [2] measured the torsional stress of the engine in a cargo vessel by using the experimental method and then determined its barred speed range. Sun et al. [3] analyzed the influence of the rotational inertia of the flywheel on the torsional vibration of compressor shafting by using the multi-body dynamics simulation method. To minimize the torsional vibration transmission between shafts adaptively to the dynamic disturbance, Lee et al. [4] designed a stiffness variable flexible coupling using magnetorheological elastomer. Based on the radial basis function (RBF) neural network and genetic algorithm (GA), Liu et al. [5] optimized the maximum the directional factor of critical modes to improve the torsional vibration of compressor shafting. To obtain the reasonable matching type of silicone oil shock absorber, Wang et al. [6] developed a

(2) Determination of optimal damping value

When the inertia ratio is determined, the optimal damping value C_d is equal to 624 N·m·s/rad according to Equation (4), and then the optimal viscous damping ratio ξ is equal to 0.3761 according to Equation (5). Generally, the value of C_d in the shock absorber is between 200-6000 and the value of ξ is between 0.02-0.63, which means that the design of torsional shock absorber meets the requirements.

$$C_d = \frac{2\omega_n J_d}{\sqrt{2(\mu+1)(\mu+2)}} \quad (4)$$

$$\xi = \frac{1}{\sqrt{2(\mu+1)(\mu+2)}} \quad (5)$$

(3) Determination of the viscosity coefficient of silicone oil

Since the silicone oil is dimethyl silicone oil, the effective viscosity can be obtained by the empirical equation as follows:

$$\nu_e = \frac{C_d b}{9.98 \times 10^{-13} \times 2\pi B R_2^3 \left(1 + \frac{R_2}{2B} \eta_R\right)} \quad (6)$$

where η_R is a damping correction coefficient determined by the ratio of the inner diameter to the outer diameter of the inertia ring and the average shear rate. According to the literature [7], when the ratio of inner diameter to outer diameter of the inertia ring is 0.6 and the average shear rate is less than 700 Rad^2 / s , η_R is equal to 0.89. According to Equation (6), the effective viscosity of silicone oil is 9.4844e4 cs or 0.0948 m^2/s .

The nominal viscosity of silicone oil can be calculated by Equation (7).

$$\nu_o = \frac{\nu_e}{\eta_v \eta_t} \quad (7)$$

where η_v is the correction coefficient for shear rate, and η_t is the temperature correction coefficient. Considering that the shock absorber is installed outside the machine and is close to the casing of the fracturing pump, the working temperature is regarded as 45°C. According to the literature [7], the nominal viscosity of silicone oil is 1.64e5 cs or 0.164 m^2/s when η_v is 0.86 and η_t is 0.67.

Due to the high power of fracturing pump, heavy vibration, and wide range of working temperature, the working temperature whose value is selected as 45°C is relatively low. However, the calculated nominal viscosity is still high. This is because the design of the inertia ring is unreasonable. In other words, the effective viscosity value is larger if the ratio of R_3 to R_2 is larger and the correction coefficient η_R is smaller. Additionally, Equation (7) shows that the thickness of the inertia ring has a significant effect on the effective viscosity.

Therefore, reducing the outer diameter R_2 of the inertia ring and increasing the thickness B of the inertia ring can be considered in further optimization design.

(4) Check for heat dissipation area

The heat dissipation area is the outer surface area of the inertia ring, whose value is 0.1937 m^2 . The energy consumed by each vibration cycle of the shock absorber has an upper limit E_d . The upper limit E_d can be calculated by Equation (8).

$$E_d = \frac{\sqrt{\mu+1}}{\mu+2} \pi J_d \omega^2 A_{eA}^2 \quad (8)$$

The relationship between energy consumed and power is shown by Equation (9).

$$W_d = \frac{\omega}{2\pi} E_d \quad (\text{W}) \quad (9)$$

According to Equation (9), the power is equal to 16.9 W and the power consumption per unit area is equal to 87.32 W/m^2 . This value is far less than 6.39 kW/m^2 , which indicates that the design is reasonable.

Finally, the design parameters of the torsional shock absorber are obtained as shown in Table 1.

Table 1 Design parameters of the torsional shock absorber

Parameters	Value	Parameters	Value
Inertial ring outer radius (mm)	165.90	Effective viscosity of silicone oil (m ² /s)	0.0948
Inertial ring inner radius (mm)	99.538	Nominal viscosity of silicone oil (m ² /s)	0.164
Inertial ring weight (kg)	21.7291	Dissipation area (m ²)	0.1937
Inertial ring rotational inertial (kg·m ²)	0.4067	Damping value (N·m·s/rad)	624
Gap of silicone oil (mm)	0.538	Outer radius of shock absorber (mm)	170.435
Inertial ring thickness (mm)	49.77	Inner radius of shock absorber (mm)	95
Inertia ratio	0.4453	Damping ratio	0.3761

3. Parameter optimization of torsional shock absorber based on PSO

In this paper, to complete the preliminary design of the torsional shock absorber with silicone oil damping, the inertia ring is designed by using the empirical method, all design parameters are calculated, and the type of silicone oil is selected. Since the inertia ratio is the most influential parameter in the entire design process, the optimal inertia ratio should be first determined according to the fixed frequency and amplitude amplification coefficient curve of the original system, and then the size of inertia ring size should be designed. Therefore, the standard particle swarm optimization (PSO) algorithm is used to optimize parameters of the torsional shock absorber to obtain better design parameters and corresponding torsional vibration response.

3.1 Particle swarm optimization

(1) Parameter settings

The parameters of PSO are provided in Table 2.

Table 2 Parameter settings of PSO

Parameters	Value	Parameters	Value
Upper limit of radius ratio	0.65	Upper limit of connection stiffness	2×10 ⁶
Lower limit of radius ratio	0.25	Lower limit of connection stiffness	1×10 ⁶
Upper limit of thickness diameter ratio	0.6	Lower speed limit	1
Lower limit of thickness diameter ratio	0.2	Lower speed limit	-1
Inertia weight w	0.6	Group dimension	3
Learning coefficient C_1	2	Particle swarm size	100
Learning coefficient C_2	2	Maximum number of iterations	500
Minimum fitness	0.01		

(2) Evaluation of each particle

The fitness values of all particles are calculated. If the fitness value of a particle is better than current global optima, the position of the particle is recorded and the current global optima is updated [8].

(3) Update of particle

The velocity of particle is updated as follows:

$$v_{id}^{t+1} = \omega v_{id}^t + c_1 r_1 (p_{id}^t - x_{id}^t) + c_2 r_2 (p_{gd}^t - x_{gd}^t) \quad (10)$$

The position of particle is updated as follows:

$$x_{id}^{t+1} = x_{id}^t + v_{id}^{t+1} \quad (11)$$

where v_{id}^t and v_{id}^{t+1} are the velocity of particle before and after the update respectively. r_1 and r_2 are both the random number distributed on $[0, 1]$. x_{id}^t and x_{id}^{t+1} are the position of particle before and after the update respectively. p_{id}^t and p_{gd}^t are the individual optimal position and the global optimal position, respectively.

During the process of updating the velocity of particle, the value of corresponding boundary is adopted if the velocity goes beyond the boundary. As can be seen from Equation (11), the participation ratio of the velocity of particle is related to the inertial weight. If the inertial weight is large, PSO has a strong global search capability; otherwise, PSO has a strong local search capability [8].

(4) Check whether the termination conditions are met.

3.2 Torsional vibration response before optimizing torsional shock absorber

According to the lumped mass parameter system of the torsional shock absorber and the original system, the lumped mass parameter model of new system can be constructed as shown in Figure 2.

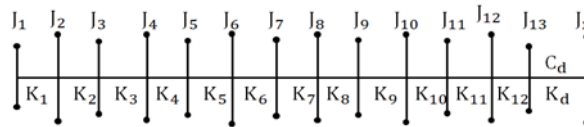


Figure 2 Lumped mass parameter model of new system

In Figure 2, J_x is the equivalent rotational inertia of the torsional shock absorber, which can be obtained by Equation (12):

$$J_x = \frac{J_d}{2} + J_h \quad (12)$$

where J_h is the rotational inertia of the sealing cover and shell ($\text{kg}\cdot\text{m}^2$); J_d is the rotational inertia of the inertia ring ($\text{kg}\cdot\text{m}^2$). As mentioned above, J_d is $0.4067 \text{ kg}\cdot\text{m}^2$, C_d is $624 \text{ N}\cdot\text{m}\cdot\text{s}/\text{rad}$, and K_d is the connection stiffness between the torsional shock absorber and the free end of the crankshaft. The connection stiffness of the torsional shock absorber has a significant impact on the torsional vibration reduction [9]. Therefore, it is necessary to calculate the amplitude of the torsional vibration response under different connection stiffness to find the optimal connection stiffness. As shown in Figure 3, different connection stiffness corresponds to different maximum torsion angles.

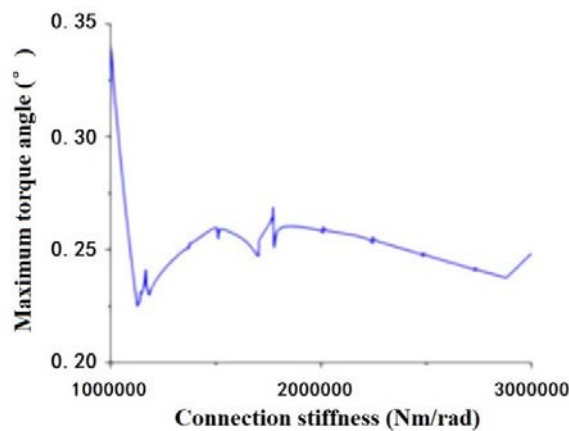


Figure 3 Maximum torsional angle under different connection stiffness

It can be concluded that the torsional shock absorber has the best effect of torsional vibration reduction when the connection stiffness is about $1.126 \times 10^6 \text{ Nm}/\text{rad}$.

The three-dimensional models of the free end of the crankshaft, the sealing cover of the torsional shock absorber, and the shell are established, and then the rotational inertias of the shell and the sealing cover are calculated as $0.179 \text{ kg}\cdot\text{m}^2$. However, the rotational inertias of the shell and the sealing cover are calculated as $0.1772 \text{ kg}\cdot\text{m}^2$ by using the numerical method. The reason for this error is that the minimum accuracy of 3D modeling software is 0.01mm . In this work, the result obtained by the numerical method is adopted. Thus, the ratio of the rotational inertia of the ring to the shell and the sealing cover is 2.295 and it is within the range of 1.25 to 2.86, which indicates the design is reasonable. According to Equation (12), we can note that the equivalent rotational inertia of the torsional shock absorber is $0.3805 \text{ kg}\cdot\text{m}^2$. When solving the torsional vibration response of the original system, the mode proportional damping is used to replace the damping of the original system, and the modal damping ratio is a constant whose value is 0.01.

The lumped mass parameter model of new system is constructed. Then, the torsional vibration responses of the free end of the crankshaft are obtained by the modal superposition method for the new system and the original system [10].

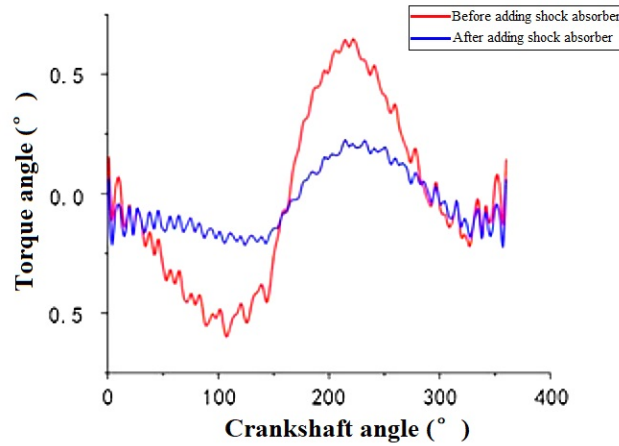


Figure 4 Comparison of responses before and after adding the torsional shock absorber

As shown in Figure 4, after adding the torsional shock absorber, the torque angle of the free end is significantly decreased, and the maximum torque angle is 0.2249° . Compared with the maximum torque angle before adding the torsional shock absorber, the maximum torque angle after adding the torsional shock absorber has decreased by 65.31%. Thus, the design of the torsional shock absorber can effectively reduce torsional vibration of the system.

3.3 Torsional vibration response after optimizing torsional shock absorber

To minimize the amplitude of the torsional vibration response, the objective function is established as shown in Equation (13).

$$\theta(t) = [u]\theta_r(t) \quad (13)$$

where $[u]$ is the modal matrix of the lumped mass parameter model.

$$\theta_r(t) = \begin{Bmatrix} \frac{1}{\omega_1^2} \left(\frac{a_{10}}{2} + \sum_{j=1}^m (|H_{1j}| (a_j \cos(j\omega t - \phi_{1j}) + b_j \sin(j\omega t - \phi_{1j}))) \right) \\ \frac{1}{\omega_2^2} \left(\frac{a_{20}}{2} + \sum_{j=1}^m (|H_{2j}| (a_j \cos(j\omega t - \phi_{2j}) + b_j \sin(j\omega t - \phi_{2j}))) \right) \\ \vdots \\ \frac{1}{\omega_n^2} \left(\frac{a_{n0}}{2} + \sum_{j=1}^m (|H_{nj}| (a_j \cos(j\omega t - \phi_{nj}) + b_j \sin(j\omega t - \phi_{nj}))) \right) \end{Bmatrix} \quad (14)$$

The PSO algorithm is executed for 30 times. The minimum amplitude of the torsional vibration response and the corresponding parameters of the torsional shock absorber are recorded in Table 3.

Table 3 Optimal parameters of the torsional shock absorber and torsional vibration response

NO.	Radius ratio	Thickness diameter ratio	Connection stiffness	Amplitude (deg)	Optimization rate (%)
1	0.55	0.28	1.78×10^6	0.2164	3.78
2	0.62	0.60	1.78×10^6	0.2164	3.78
3	0.54	0.25	1.78×10^6	0.2164	3.78
4	0.54	0.26	1.78×10^6	0.2164	3.78
5	0.60	0.50	1.78×10^6	0.2164	3.78
6	0.59	0.45	1.78×10^6	0.2164	3.78
7	0.59	0.47	1.78×10^6	0.2164	3.78
8	0.54	0.25	1.78×10^6	0.2164	3.78
9	0.57	0.34	1.78×10^6	0.2164	3.78
10	0.60	0.51	1.78×10^6	0.2164	3.78
11	0.61	0.57	1.78×10^6	0.2164	3.78
12	0.60	0.48	1.78×10^6	0.2164	3.78
13	0.60	0.48	1.78×10^6	0.2164	3.78
14	0.58	0.43	1.79×10^6	0.2112	6.09
15	0.56	0.32	1.78×10^6	0.2103	6.49
16	0.57	0.31	1.78×10^6	0.2103	6.49
17	0.52	0.20	1.78×10^6	0.2103	6.49
18	0.61	0.58	1.78×10^6	0.2103	6.49
19	0.61	0.54	1.78×10^6	0.2103	6.49
20	0.61	0.58	1.78×10^6	0.2103	6.49
21	0.58	0.39	1.78×10^6	0.2103	6.49
22	0.58	0.39	1.78×10^6	0.2103	6.49
23	0.57	0.38	1.78×10^6	0.2103	6.49
24	0.57	0.35	1.78×10^6	0.2103	6.49
25	0.54	0.26	1.78×10^6	0.2103	6.49
26	0.62	0.59	1.78×10^6	0.2103	6.49
27	0.62	0.60	1.78×10^6	0.2103	6.49
28	0.61	0.55	1.78×10^6	0.2103	6.49
29	0.53	0.22	1.78×10^6	0.2103	6.49
30	0.54	0.25	1.78×10^6	0.2103	6.49

As can be seen from Table 3, there are 13 optimization rate of 3.78%, one optimization rate of 6.09%, and 16 optimization rate of 6.49%. Compared with the torsional vibration response before adding the torsional shock absorber, the torsional vibration response after adding the optimal torsional shock absorber has decreased by 66.02%.

Considering that the nominal viscosity of silicone oil and the effective viscosity of silicone oil are relatively high in the preliminary design, the result that the inertia ring has a larger thickness is selected from the 16 optimal results. Among these results, the parameters in groups 18, 19, 20, 26, 27, and 28 meet the design requirement.

The damping effect of the optimal torsional shock absorber is significantly enhanced, which proves that the parameter optimization of the torsional shock absorber based on PSO algorithm is effective and feasible.

4. Conclusions

According to the structure of fracturing pump crankshaft system, the torsional shock absorber with silicone oil damping is designed in this paper. The inertia ratio, optimal damping value, nominal viscosity, heat dissipation area, and other design parameters are obtained in detail. Moreover, the crucial parameters of the torsional shock absorber are optimized by using the standard PSO algorithm. The torsional vibration responses of the system before and after optimizing torsional shock absorber are calculated and compared with those of the original system. The statistical results indicate that the torsional shock absorber has a significant suppression effect on torsional vibration of the system, and the suppression effect is improved by using optimal torsional shock absorber.

Acknowledgements

The authors gratefully acknowledge the financial support from High-Tech Ship Scientific Research Project of Ministry of Industry and Information Technology of China "Research on Key Technologies of Deep-Water Fracturing Ship".

References

- [1] Wu Lei, Xiao Wensheng, Liu Zhongyan, Xiao Liusheng. Research and improvement of fracturing truck frame configuration [J]. Computer Simulation, 2014, 031(7): 103-106.
- [2] Zhu jianyuan, Wu Qijing. Research on the torsional vibration characteristics and the speed restricted range of running ship [J]. Mechanical & Electrical Equipment, 2010, 27(4): 21-23+35.
- [3] Sun Xiaodong, Liu Jian, Cao Hu, et al. Torsional vibration characteristics analysis of the reciprocating compressor's crankshaft system [J]. China Petroleum Machinery, 2017, 45(8): 61-64.
- [4] LEE K H, PARK J E, KIM Y K. Design of a stiffness variable flexible coupling using magnetorheological elastomer for torsional vibration reduction [J]. Journal of Intelligent Material Systems and Structures, 2019, 30(15): 2212-2221.
- [5] Liu Jian, Sun Xiaodong, Hou xiaobing, et al. Multi-objective optimization design of structural parameters of compressor fully balanced crankshaft [J]. Machine Design & Manufacturing, 2019(2): 58-61.
- [6] Wang Fengqin, Wang Huan, Xiao Nengqi. Matching optimization of silicone oil shock absorber parameter for marine diesel engine propulsion system [J]. Ship Engineering, 2018, 40(9): 32-37.
- [7] Guidelines for inspection of silicone oil shock absorbers for marine diesel engines [G], China Classification Society, 2007.
- [8] KENNEDY J, EBERHART R. Particle swarm optimization [C], in: Proceedings of ICNN'95 - International Conference on Neural Networks, 1995, pp. 1942-1948 vol.1944.
- [9] Yan Weiming, Wang Jin, Xu Weibing, et al. Influences of connected rigidity on vibration control effect of tuned particle dampers [J]. Journal of Vibration and Shock, 2018.

[10] Xu Youlin, Li Qi, Wu Dingjun, et al. Stress and acceleration analysis of coupled vehicle and long-span bridge systems using the mode superposition method [J]. *Engineering Structures*, 2010, 32(5):1356-1368